On the Role of Joule Heating as a Source of Gravity-Wave Energy above 100 km

WILLIAM BLUMEN

Dept. of Astro-Geophysics, University of Colorado, Boulder

AND RICHARD G. HENDL[1]

Air Force Cambridge Research Laboratories, Bedford, Mass.

(Manuscript received 26 August 1968)

ABSTRACT

Observations of ionospheric disturbances by various investigators have led to the suggestion that auroral energy may be coupled to atmospheric wave motions through joule heating. A linear model of internal gravity-wave generation by joule heating in the region of the auroral electrojet (100–150 km above the earth's surface) is investigated. Heat conduction, viscosity and reflection of wave energy by atmospheric inhomogeneities are not considered. The computed value of the upward wave-energy flux from the source region is of order 0.1–1 erg cm^{-2} sec^{-1} and is of sufficient magnitude to be of importance in the energetics of the F region. Shortcomings of the present model are discussed, with emphasis on how the physical features which have been neglected might affect the present results.

1. Introduction

Hines (1965) has suggested that dynamical heating of the lower ionosphere by viscous dissipation of propagating gravity waves could produce temperature increases of between 10K day^{-1} (near 95 km) and 100K day^{-1} (near 140 km). It is further suggested that these propagating waves transfer energy to the regions above 140 km and, in conjunction with solar radiation, provide the necessary heating requirements of the F region. Hines' estimate of the wave-energy flux across the 140-km level to the overlying region is of order 0.1–1 erg cm^{-2} sec^{-1}.

Speculation concerning the sources for the generation of traveling ionospheric wave motions abound in the literature. There is evidence to indicate that waves generated in the troposphere (e.g., mountain waves) could penetrate to ionospheric heights (Friedman, 1966), and Lindzen's (1967) computations suggest that the upward flux of diurnal tidal energy from the mesosphere may be an important factor in the energetics of the ionosphere. However, the vertical stratification of wind and temperature in the atmosphere is responsible for a selective reflection which could, in some instances, prevent a significant amount of the energy of some wave components from reaching the ionosphere. Irrespective of how much wave energy eventually reaches the ionosphere from regions below, it seems reasonable to expect that *in situ* sources of wave energy should play a significant role in the energetics of the ionosphere.

Observations of traveling ionospheric disturbances emanating from polar regions has led to the suggestion that auroral energy may be coupled to atmospheric wave motions through heating produced by ohmic dissipation of electric currents, joule heating (e.g., Hines, 1965; King, 1966). Cole's (1962) pioneer work has established that joule heating in the region 100–200 km could lead to large temperature changes, through heat flux by thermal conduction in the vicinity of 150 km and above. However, below 150 km it appears that the relaxation time, i.e., the time it takes an initial temperature impulse T_i to fall to $e^{-1}T_i$, is at least one day and is independent of T_i (Thomas, 1967). On this basis short-period gravity waves ($\sim$1 hr) should transfer energy more efficiently than conduction below about 150 km, if the vertical scale of the propagating waves is approximately greater than the local scale height (Pitteway and Hines, 1963; Hines, 1964) and if the coupling of auroral heating into gravity wave energy is efficient. Above 150 km viscous dissipation of wave energy and thermal conduction undoubtedly become increasingly important.

The present analysis is designed to focus attention on the important parameters associated with energy flux, by internal gravity waves, from the region of maximum joule heating in the auroral zone, and to provide an estimate of the magnitude of this flux. For this purpose, a relatively simple model containing joule heating above 100 km is used. The range of parameters which describe the spatial and temporal distribution of electric currents and the magnitude of the associated heating are presented in Section 2. In Section 3 a scale analysis is used to establish the maximum heating rate which may be

[1] Captain, U. S. Air Force.

TABLE 1. General features of the auroral electrojet.

Feature	Investigator	Method of determination
Height of jet axis (km)†		
115	Boström (1964)	Theoretical model
100–150	Nagata (1950)	Magnetogram
100–140	Belon *et al.* (1966)	Photometric triangulation
Length (km)‡		
2000	Nagata (1962)	All sky camera
5000	Akasofu (1963)	All sky camera
North-south thickness (km)		
500	Nagata (1962)	All sky camera
680	Scrase (1967)	Magnetogram
Vertical half-width (km)		
30	Boström (1964)	Theoretical model
Current density (A m^{-2})		
3×10^{-5}	Cole (1962)	Theoretical model
1.2×10^{-4}	Boström (1964)	Theoretical model
Duration (min)		
<60	Heppner (1954)	Magnetogram
~30	Akasofu (1964)	Magnetogram and all sky camera.

† Also height of maximum joule heating.
‡ Measured along an auroral arc which is oriented approximately in the magnetic east-west direction.

used in order to treat the analysis within the framework of linear theory. It is tacitly assumed that all the available heat energy is entirely coupled into gravity wave energy. Then the vertical energy flux is computed in Section 4, where it is shown that fluxes of 0.1–1 erg cm^{-2} sec^{-1} may be obtained for characteristic values of the geometry and duration of the heating. The shortcomings of the present model are discussed in conjunction with suggestions for further work in Section 5

2. Auroral electrojet

Intense electric currents associated with polar magnetic disturbances, called electrojets, are known to flow in the auroral oval (Akasofu *et al.*, 1965). A morphology of the aurora and associated electrojet may be found in the review papers by Akasofu (1965) and Akasofu *et al.* (1965). Here we shall be concerned with presenting a brief survey of the important parameters associated with the electrojet, which have been presented by a number of investigators.

General features of the auroral electrojet which are useful for present purposes are presented in Table 1. The north-south thickness in the table refers to a broad sheet current containing intense local currents, wherever there are auroral arcs (Rees and Walker, 1968). The thickness of the individual arcs may be a fraction of a kilometer or a few tens of kilometers (Kim and Volkman, 1963; Maggs and Davis, 1968). The duration of time (<60 min) refers to the period when the enhanced current (electrojet) flows, but weaker currents may flow for periods of a few hours (Scrase, 1967).

Although some information from theoretical models has been presented in Table 1, most of the information concerning the spatial and temporal distribution of the electrojet has been inferred from measurements during geomagnetic activity by various methods. However, it is not possible to determine whether the most intense currents were flowing during periods when these measurements were made. It should also be pointed out that the spatial and temporal distributions of the electrojet could differ from the values in Table 1 if another magnetic disturbance occurs before the preceding event has been completed. In this case the current distribution could be quite variable in space and time.

The orientation of the electric field **E** in the ionosphere which drives the auroral electrojet has still not been determined. The orientation of **E** relative to the electrojet determines whether the current is primarily a Pedersen current (parallel to **E**) or a Hall current (normal to **E**). This distinction is important for our purposes, since only the Pedersen current determines the joule heating rate (e.g., Cole, 1962). This heating rate associated with the auroral electrojet has been estimated to have an amplitude of about 10^{-5} erg cm^{-3} sec^{-1} in the region between 100 and 150 km (Cole, 1962; Rees and Walker, 1968).

3. Scale analysis and linearization

In the following we shall determine an upper bound on the amplitude of the joule heating, in order to treat the problem of gravity wave generation within the framework of linear theory. In the atmosphere below about 150 km heat conduction and viscosity will be neglected. The neglect of viscosity and thermal conduc-

tion may be a tenuous approximation since Hines (1964) has estimated that only waves whose vertical wavelength is roughly greater than a scale height are essentially unaffected by these dissipative processes below 150 km.

The variation of heating along the electrojet is not well-established and, although there is evidence of pulsating currents flowing in the westward direction (Asasofu *et al.*, 1965), the current will be considered as uniform in the magnetic east-west direction (x axis). All the spatial variability is assumed to occur in a meridional plane (y,z plane).

The heating rate per unit volume due to joule heating will be denoted by Q^*. Then the first law of thermodynamics may be written

$$\rho^*\left(\frac{\partial}{\partial t}+v^*\frac{\partial}{\partial y}+w^*\frac{\partial}{\partial z}\right)\ln\theta^*=(c_pT^*)^{-1}Q^*, \qquad (3.1)$$

where ρ^* and T^* are density and absolute temperature, θ^* the potential temperature (e.g., Hess, 1959), (v^*,w^*) the (y,z) components of velocity, and c_p the specific heat at constant pressure.

The thermodynamic equation (3.1) may be nondimensionalized by introducing

$$\left.\begin{aligned}(v^*,w^*)&=D\tau^{-1}(v',w')\\ \theta^*&=\theta_0(z)(1+\theta')\\ t&=\tau t'\\ (y,z)&=D(y',z')\\ Q^*&=\alpha Q'\end{aligned}\right\}, \qquad (3.2)$$

where the primed variables are nondimensional, D and τ represent length and time scales characteristic of the heat source, $\theta_0(z)$ denotes the value of θ^* in a standard atmosphere and α is the amplitude of Q^*. For simplicity we consider $D\sim 30$ km as the characteristic depth. Had we introduced a separate scale characteristic of the horizontal dimension the following results would not be altered.

Introduction of the gas law

$$p^*=R\rho^*T^*, \qquad (3.3)$$

where R denotes the gas constant for dry air, permits us to write (3.1) as

$$\left(\frac{\partial}{\partial t'}+v'\frac{\partial}{\partial y'}\right)\ln(1+\theta')+w'\left[D\frac{d}{dz}\ln\theta_0+\frac{\partial}{\partial z'}\ln(1+\theta')\right]=\frac{\alpha R\tau}{c_pp^*}Q'. \qquad (3.4)$$

We now require that the nondimensional amplitude of the heating satisfy

$$\alpha'\equiv\alpha R\tau(c_pp^*)^{-1}\lesssim 10^{-1}. \qquad (3.5)$$

TABLE 2. Amplitude of the joule heating.

Duration of heating (min)	α(10^{-5} erg cm^{-3} sec^{-1})
10	4.27
30	1.42
60	0.71

In order to evaluate the magnitude of the heating amplitude α in (3.5), the maximum joule heating will be taken at 110 km above the earth's surface. Table 2 displays the values of α for various characteristic periods τ with $p^*=7.35\times10^{-2}$ dyn cm^{-2} (U. S. Standard Atmosphere, 1962).

If all nondimensional variables in (3.4) are expanded in a power series in α', the first-order expression in α' is the linear equation

$$\frac{\partial\theta_1'}{\partial t'}+w_1'D\frac{d}{dz}\ln\theta_0=Q', \qquad (3.6)$$

since $Dd(\ln\theta_0)/dz\sim O(1)$. Similarly, the equations of momentum and mass continuity reduce to linear equations if the amplitude of the heating is restricted by (3.5). If the estimate of 10^{-5} erg cm^{-3} sec^{-1} is a characteristic value of joule heating by the auroral electrojet, then the restriction on the magnitude of α, for the linearization to be valid, is not severe if the peak heating occurs in the vicinity of 110 km. However, if the peak heating occurs at higher levels, the maximum allowable value of α decreases with the pressure.

4. Energy flux

In order to determine the energy flux from a region of nonuniform joule heating within the auroral zone, we shall assume that (3.5) is satisfied and use a linear model. The equations of this model have already been used by Maeda and Watanabe (1964) in their study of infrasonic waves associated with geomagnetic activity. In dimensional form, this system of equations governing perturbation motion superposed on a resting, hydrostatic and isothermal atmosphere is:

$$\frac{\partial v}{\partial t}=-\frac{\partial p}{\partial y}, \qquad (4.1)$$

$$\frac{\partial w}{\partial t}=-\left(\frac{\partial}{\partial z}+\Gamma\right)p+g\theta, \qquad (4.2)$$

$$\frac{\partial}{\partial t}\frac{p}{c^2}+\frac{\partial v}{\partial y}+\frac{\partial w}{\partial z}-\Gamma w=s, \qquad (4.3)$$

$$\frac{\partial}{\partial t}g\theta+N^2w=gs. \qquad (4.4)$$

The first-order quantities which appear in (4.1)–(4.4) are defined by the transformations

$$\rho_0^{\frac{1}{2}}(v_1^*,w_1^*)=(v,w),\ \rho_0^{-\frac{1}{2}}p_1^*=p,\ \rho_0^{\frac{1}{2}}\theta_0^{-1}\theta_1^*=\theta, \quad (4.5)$$

where ρ_0 denotes the basic-state density distribution in an isothermal atmosphere and the starred variables are first-order velocity (v_1^*,w_1^*), pressure p_1^* and potential temperature θ_1^*. The parameters are defined as

$$\Gamma\equiv\frac{g}{c^2}+\frac{1}{2}\frac{d}{dz}\ln\rho_0=(1/\gamma-\tfrac{1}{2})/H, \quad (4.6)$$

$$N^2=g\frac{d}{dz}\ln\theta_0, \quad (4.7)$$

$$c^2=\gamma RT_0, \quad (4.8)$$

where γ denotes the ratio of the specific heats and $H=RT_0/g$ is the scale height. The physical interpretation of Γ, N (the Brunt-Väisälä frequency) and c (the adiabatic sound speed) are discussed by Eckart (1960). Finally, the transformed heating function is

$$s(y,z,t)=\rho_0^{-\frac{1}{2}}(c_pT_0)^{-1}Q^*. \quad (4.9)$$

Since the characteristic period of the imposed heating is assumed to be $\tau\sim10^3$ sec, little energy should appear in the high frequency internal acoustic modes whose maximum period is $\tau\sim300$ sec. For that reason we shall eliminate acoustic waves entirely by setting $\partial(p/c^2)/\partial t=0$ in (4.3). With this approximation, it may be shown that the system of equations (4.1)–(4.4) only describes the motion field of internal gravity waves (e.g., Ogura and Phillips, 1962).

The energy equation may be derived by multiplying (4.1)–(4.4) by v, w, p and $g\theta$, respectively, and adding the resulting equations, to obtain

$$\frac{\partial}{\partial t}\epsilon=-\left(\frac{\partial}{\partial y}pv+\frac{\partial}{\partial z}pw\right)+(p+g^2\theta)s, \quad (4.10)$$

where

$$\epsilon=\tfrac{1}{2}[v^2+w^2+(g\theta/N)^2] \quad (4.11)$$

denotes the sum of kinetic plus available potential wave energy per unit volume. Integration over all time t and horizontal space y, denoted by a bar, yields

$$d(\overline{pw})/dz=\overline{(p+g^2\theta)s}, \quad (4.12)$$

assuming that all variables approach zero sufficiently rapidly at infinity in time and space. In the source region, $s\neq0$ in $z_1\leq z\leq z_2$, the divergence of the total wave energy flux is given by (4.12). Below the source region, $z<z_1$, $\overline{pw}=$constant. If the lower boundary is a rigid horizontal surface on which $w=0$, then $\overline{pw}$ must vanish for $z<z_1$. This means that the total energy flux directed downward is totally reflected. Above the source region, $z>z_2$, the net upward directed energy flux $\overline{pw}=$constant. It is this constant upward flux which we want to determine.

If all the variables but w are eliminated from (4.1)–(4.4), we obtain

$$\left[\frac{\partial^2}{\partial t^2}\left(\frac{\partial^2}{\partial z^2}-\Gamma^2\right)+\left(\frac{\partial^2}{\partial t^2}+N^2\right)\frac{\partial^2}{\partial y^2}\right]w=\left[\left(\frac{\partial}{\partial z}+\Gamma\right)\frac{\partial^2}{\partial t^2}+g\frac{\partial^2}{\partial y^2}\right]s. \quad (4.13)$$

In order to solve (4.13), $s(y,z,t)$ must be specified. For simplicity we shall assume that the space and time distributions are independent of each other and write (4.9) as

$$s(y,z,t)=\beta s_1(z)s_2(y)s_3(t), \quad (4.14)$$

where

$$\beta\equiv\rho_0^{-\frac{1}{2}}(z_1)(c_pT_0)^{-1}\alpha \quad (4.15)$$

denotes the amplitude of $s(y,z,t)$, z_1 is the height at which the heating is a maximum, and the factor $\exp[-(z-z_1)/2H]$, from the variable $\rho_0^{\frac{1}{2}}(z)$, has been absorbed in $s_1(z)$. On the basis of ground level magnetic records various authors (e.g., Cole, 1962; Scrase, 1967) have suggested that the current amplitude falls off smoothly in the north and south directions. Further, the period of maximum heating has been estimated to be an hour or less (Table 1), but its variability during this period is unknown.

For the purposes of the present model we shall assume that $Q^*\propto\exp[-(z-z_1)/2H]$ over a finite depth. Accordingly, $s_1(z)$ takes the form

$$\left.\begin{aligned}s_1(z)&=1, \quad z_2\geqslant z\geqslant z_1\\ s_1(z)&=0, \quad z>z_2,\ z<z_1\end{aligned}\right\}. \quad (4.16)$$

The distribution along the y axis is given by

$$s_2(y)=\frac{a^2}{a^2+y^2}, \quad -\infty\leq y\leq\infty, \quad (4.17)$$

where a dentoes the heating half-width. The distribution in time will be represented by

$$s_3(t)=\pi^{-1}\sin^2(t/T)/(t/T)^2, \quad -\infty\leq t\leq\infty, \quad (4.18)$$

where T is a constant. Although the distribution with respect to y and t extend to infinity, over 90% of the heating is concentrated within the range y/a and t/T equal to $\pm\pi$.

A Fourier transform with respect to y and t reduces (4.13) to

$$\left(\frac{d^2}{dz^2}-\mu^2\right)W(z;k,\sigma)=\left(\frac{d}{dz}+\Gamma+\frac{gk^2}{\sigma^2}\right)S(z;k,\sigma), \quad (4.19)$$

where

$$\left.\begin{aligned} W(z;k,\sigma)&=\frac{1}{4\pi}\int_{-\infty}^{\infty}\int_{-\infty}^{\infty}w(y,z,t)e^{-i(ky+\sigma t)}dydt\\ S(z;k,\sigma)&=\frac{1}{4\pi}\int_{-\infty}^{\infty}\int_{-\infty}^{\infty}s(y,z,t)e^{-i(ky+\sigma t)}dydt\end{aligned}\right\}, \quad (4.20)$$

$$\mu\equiv\left[\frac{(\sigma^2-N^2)k^2+\sigma^2\Gamma^2}{\sigma^2}\right]^{\frac{1}{2}}. \quad (4.21)$$

For an isothermal atmosphere at temperature T_0, (4.19) has constant coefficients and may be solved by standard analytical methods. The solution of (4.19), which has been obtained by Mackie (1965, p. 48), for example, is

$$W(z;k,\sigma)=-\hat{S}\left\{\mu^{-1}e^{-\mu z}\int_0^z\sinh(\mu\xi)s_1(\xi)d\xi+\mu^{-1}\sinh(\mu z)\int_z^{\infty}e^{-\mu\xi}s_1(\xi)d\xi\right\}, \quad (4.22)$$

where

$$\hat{S}\equiv\beta S_2(k)S_3(\sigma)(\Gamma+gk^2/\sigma^2). \quad (4.23)$$

The integrals in (4.22) may be evaluated if the distribution $s_1(z)$ in (4.16) is used. However, since the energy flux will be evaluated in the region $z>z_2$ we need only consider the solution

$$W(z;k,\sigma)=-\hat{S}\mu^{-1}e^{-\mu z}\int_{z_1}^{z_2}\sinh(\mu\xi)d\xi. \quad (4.24)$$

Upon integration, (4.24) becomes

$$W(z;k,\sigma)=-\tfrac{1}{2}\hat{S}\mu^{-2}\{e^{-\mu(z-z_2)}+e^{-\mu(z+z_2)}-e^{-\mu(z-z_1)}-e^{-\mu(z+z_1)}\}. \quad (4.25)$$

The pressure p may be obtained by combining (4.1) and (4.3) to obtain

$$\frac{\partial}{\partial t}\left(\frac{\partial}{\partial z}-\Gamma\right)w=\frac{\partial^2 p}{\partial y^2}. \quad (4.26)$$

The Fourier transform with respect to y and t yields

$$P(z;k,\sigma)=-\frac{i\sigma}{k^2}\left(\frac{d}{dz}-\Gamma\right)W(z;k,\sigma). \quad (4.27)$$

The straightforward but lengthy computation of the total upward energy flux emanating from the source region is described in Appendix A. The result is

$$\overline{pw}=16\pi^2\beta^2\int_0^{\infty}|S_2(k)|^2\int_0^{Nk(k^2+\Gamma^2)^{-\frac{1}{2}}}\frac{\sigma}{k^2\lambda^3}|S_3(\sigma)|^2\times\left(\Gamma+\frac{gk^2}{\sigma^2}\right)^2[1-\cos\lambda(z_1+z_2)]\times[1-\cos\lambda(z_2-z_1)]d\sigma dk, \quad (4.28)$$

where

$$\lambda=-i\mu. \quad (4.29)$$

The negative sign has been used in (4.29) to insure that only waves which transport energy upward away from the source are included in the solution (Eliassen and Palm, 1961). We note that the upward flux of energy depends on the phase of each internal wave relative to the distance between the source region and the ground surface and relative to the vertical extent of the source region itself. Consider the factor

$$1-\cos\lambda(z_2-z_1)=1-\cos 2\pi L_z^{-1}(z_2-z_1), \quad (4.30)$$

where L_z denotes vertical wavelength. For example, there is no contribution to the energy flux for the wave in which $L_z=z_2-z_1$, because nodal surfaces occur at z_2 and z_1 and no work is done at the boundaries of the source region. Similar arguments apply for other phase relationships.

The integration over σ and k in (4.28) is described in Appendix B. It has been found that if $a/H\gtrsim 6$ ($H\sim 8$ km at $z=110$ km), the energy flux is represented quite accurately by its asymptotic value for large a and is given by (B9). This is sufficient for our purposes since the north-south thickness of the electrojet has been estimated to be the order of hundreds of kilometers (Table 1). In order to obtain an estimate of the vertical flux of energy through a unit horizontal area in a unit time, $\overline{pw}$ has been divided by the "effective widths"

$$2\pi a=2\int_{-\infty}^{\infty}\frac{a^2}{a^2+y^2}dy, \quad (4.31)$$

$$2\pi T=2\int_{-\infty}^{\infty}\frac{\sin^2(t/T)}{(t/T)^2}dt. \quad (4.32)$$

The nondimensional energy flux

$$(\overline{pw}/4\pi^2 aT)/(\beta^2N^2T/2\pi\Gamma^3)$$

is shown in Fig. 1 as a function of $z_2-z_1\equiv\Delta Z$ for indicated values of $2\pi a$ and $2\pi T$. When $2\pi T=10$ min, the energy flux is essentially independent of a and is given by (B9) with the term proportional to $NT/(4\Gamma a)$ neglected.

The following values, used in the construction of Fig. 1, are characteristic of $z\sim 110$ km (U. S. Standard

Atmosphere, 1962):

$$T_0 \sim 257\text{K}$$
$$\rho_0 \sim 9.83\times10^{-11}\ \text{gm cm}^{-3}$$
$$g \sim 948\ \text{cm sec}^{-2}$$
$$N^2 \sim 3.5\times10^{-4}\ \text{sec}^{-2}$$
$$\Gamma \sim 2.7\times10^{-7}\ \text{cm}^{-1}.$$

The characteristic values of $\beta^2N^2T/(2\pi\Gamma^3)$ corresponding to the values of α in Table 2, are approximately 5.0, 1.6 and 0.8 erg cm^{-2} sec^{-1} for $2\pi T=10$, 30 and 60 min, respectively.

On the basis of the present computations it appears that an upward flux of 0.1–1.0 erg cm^{-2} sec^{-1} could be realized from joule heating during auroral activity. In order to determine the fraction of the total energy which is transported upward, the ratio

$$E\equiv\overline{pw}\Big/\int_{z_1}^{z_2}\int_{-\infty}^{\infty}\int_{-\infty}^{\infty}Q^*dtdydz \qquad (4.33)$$

has been computed. The heating rate is given by

$$Q^*=\alpha e^{-(z-z_1)/2H}s_2(y)s_3(t), \qquad (4.34)$$

where $s_2(y)$ and $s_3(t)$ are given by (4.17) and (4.18), respectively. E as a function of ΔZ is displayed in Fig. 2. It should be noted that, since there is no net downward energy flux in the present model, $1-E$ represents the fraction of energy transported horizontally.

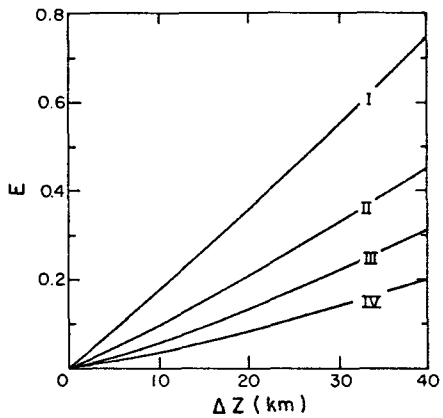

FIG. 2. Fraction of the total energy E transported upward defined by (4.33), as a function of ΔZ. The values of $2\pi a$ and $2\pi T$ corresponding to I, II, III and IV are given in Fig. 1.

5. Concluding remarks

The present investigation has been concerned with establishing the relative importance of auroral heating as a thermospheric energy source. Although the present estimate of the energy flux from the region of auroral zone heating is significant, in terms of the energy requirements of the F region, some important physical features have been omitted from the present model which could affect the propagating waves. As a first approximation, a stationary isothermal atmosphere was used to eliminate the mathematical complications which would arise from reflecting layers above and below the source region due to vertical variations of wind and temperature. It has been pointed out that the energy flux depends on the phase of each internal wave relative to the distance between the source and the perfectly reflecting ground surface. In the present case this phase relationship has a negligible effect on the magnitude of the energy flux. However, if the surface of a reflecting layer were closer to the source region (e.g., mesopause), the phase relationships of the reflected waves may have an appreciable effect on the net energy flux.

Upper level wind and temperature variations could also produce wave guides which would channel energy horizontally before it is dissipated at upper levels by viscosity. Furthermore, the levels at which propagating waves are strongly affected by viscosity depends on their vertical structure (Hines, 1964). Therefore, the relationship between the structure of the waves generated and the frequency and wavenumber spectrum of actual sources of wave energy must be established before the details of wave propagation from the auroral zone can be understood.

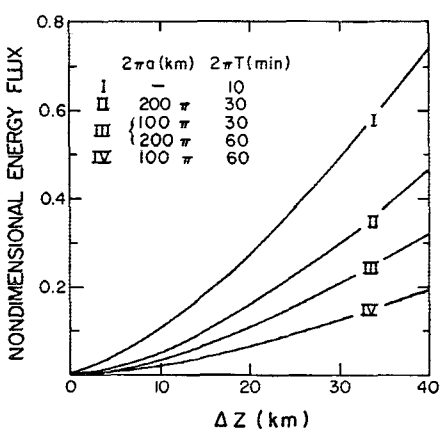

FIG. 1. Nondimensional energy flux $(\overline{pw}/4\pi^2aT)/(\beta^2N^2T/2\pi\Gamma^8)$ as a function of z_2-z_1, $\equiv\Delta Z$. Over 90% of the heating is contained within the "effective widths" $2\pi a$ and $2\pi T$.

Acknowledgments. The present paper is based on a study initially conducted by Hendl (1968). We are grateful to Drs. M. H. Rees, C. A. Reddy and Prof. T. W. Speiser for their helpful comments during the course of this investigation.

APPENDIX A

Evaluation of the Energy Flux

The vertical velocity w and the pressure p may be obtained by taking the inverse transforms of (4.25) and

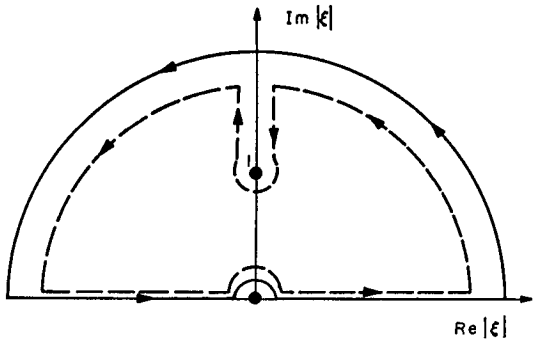

FIG. 3. Paths of integration in the ξ plane for the integrals in (B6). The solid and dashed contours correspond to the paths where $\xi=i$ is a pole and branch point, respectively.

(4.27). The real parts of these expressions are

$$\mathrm{Re}w=\frac{1}{2}\int_{-\infty}^{\infty}\int_{-\infty}^{\infty}\{AF(\lambda,Z_i)e^{i(ky+\sigma t)} +A^*F^*(\lambda,Z_i)e^{-i(ky+\sigma t)}\}dkd\sigma, \quad (A1)$$

and

$$\mathrm{Re}p=\frac{1}{2}\int_{-\infty}^{\infty}\int_{-\infty}^{\infty}\{BF(\lambda,Z_i)e^{i(ky+\sigma t)} +B^*F^*(\lambda,Z_i)e^{-i(ky+\sigma t)}\}dkd\sigma. \quad (A2)$$

The notation used is

$$A\equiv\tfrac{1}{2}\lambda^{-2}\hat{S}(k,\sigma), \quad (A3)$$

$$B\equiv\sigma/2(k\lambda)^{-2}(\lambda+i\Gamma)\hat{S}(k,\sigma), \quad (A4)$$

[where $\hat{S}$ is defined by (4.23) and λ by (4.29) and (4.21)]

$$F(\lambda,Z_i)\equiv e^{i\lambda Z_1}+e^{i\lambda Z_2}-e^{i\lambda Z_3}-e^{i\lambda Z_4}, \quad (A5)$$

where $Z_1=z-z_2$, $Z_2=z+z_2$, $Z_3=z-z_1$, $Z_4=z+z_1$, and the starred variables are complex conjugates.

The next step is to multiply (A1) and (A2) together, integrate this product over all y and t and use the expression

$$\delta(k\pm k')\delta(\sigma\pm\sigma') =(2\pi)^{-2}\int_{-\infty}^{\infty}\int_{-\infty}^{\infty}e^{i[(k\pm k')y+(\sigma\pm\sigma')t]}dydt, \quad (A6)$$

where δ denotes the Dirac delta function. The resulting expression for the energy flux is

$$\overline{pw}=4\pi^2\int_{-\infty}^{\infty}\int_{-Nk(k^2+\Gamma^2)^{-\frac{1}{2}}}^{Nk(k^2+\Gamma^2)^{-\frac{1}{2}}}(\sigma/k^2\lambda^3)|\hat{S}|^2\{1+\tfrac{1}{2}[\cos2\lambda z_2 +\cos2\lambda z_1]-\cos\lambda(z_2-z_1)-\cos\lambda(z_1+z_2)\}d\sigma dk, \quad (A7)$$

where we have used

$$\left.\begin{aligned}\lambda(\sigma,k)&=-\lambda(-\sigma,-k)\\ \hat{S}^*(-k,-\sigma)&=\hat{S}(\sigma,k)\\ \hat{S}^*(k,\sigma)&=\hat{S}(-k,-\sigma)\end{aligned}\right\}, \quad (A8)$$

and the integration over σ only extends over the spectrum of waves which transport energy vertically. Substitution of

$$\tfrac{1}{2}[\cos2\lambda z_2+\cos2\lambda z_1]=\cos\lambda(z_1+z_2)\cos\lambda(z_2-z_1) \quad (A9)$$

and (4.23) into (A.7), noting that the integrand is an even function of k and σ, yields the energy flux (4.28).

APPENDIX B

Evaluation of the Integrals

The Fourier transforms of (4.17) and (4.18) yield

$$S_2(k)=ae^{-ka}, \quad (B1)$$

and

$$\left.\begin{aligned}S_3(\sigma)&=(2\pi)^{-1}T(1-\sigma T/2), && \sigma T/2\leq 1\\ &=0, && \sigma T/2>1\end{aligned}\right\}. \quad (B2)$$

If the evaluation of (4.28) is carried out with $S_2(k)$ and $S_3(\sigma)$, given by (B1) and (B2), then the upper limit of the k integration becomes $k=2\Gamma[(NT)^2-4]^{-\frac{1}{2}}$.

The integration over σ in (4.28) is expedited by using the transformations

$$[1-\cos\lambda(z_1+z_2)][1-\cos\lambda(z_2-z_1)] =4\sin^2[\lambda(z_1+z_2)/2]\sin^2[\lambda(z_2-z_1)/2], \quad (B3)$$

$$\sigma=Nk\cos\phi(k^2+\Gamma^2)^{-\frac{1}{2}}, \quad (B4)$$

where

$$\phi=\tan^{-1}\xi. \quad (B5)$$

Substitution of (B.1)–(B.5) into (4.28) yields

$$\overline{pw}=(8\pi\beta Na)^2\int_0^{2\Gamma[(NT)^2-4]^{-\frac{1}{2}}}(k^2+\Gamma^2)^{-\frac{1}{2}}e^{-2ka} \times\int_0^{\infty}G(k,\xi)|S_3(k,\xi)|^2\sin^2[\tfrac{1}{2}(z_2-z_1)(k^2+\Gamma^2)^{\frac{1}{2}}\xi] \times\sin^2[\tfrac{1}{2}(z_1+z_2)(k^2+\Gamma^2)^{\frac{1}{2}}\xi]\xi^{-2}(1+\xi)^{-2}d\xi dk, \quad (B6)$$

where

$$G(k,\xi)\equiv\Gamma^2+2g\Gamma N^{-2}(k^2+\Gamma^2)(1+\xi^2) +(gN^{-2})^2(k^2+\Gamma^2)^2(1+\xi^2)^2, \quad (B7)$$

$$|S_3(k,\xi)|^2=(T/2\pi)^2[1-NTk(k^2+\Gamma^2)^{-\frac{1}{2}}(1+\xi^2)^{-\frac{1}{2}} +(NTk/2)^2(k^2+\Gamma^2)^{-1}(1+\xi^2)^{-1}]. \quad (B8)$$

The integration over ξ in (B6) consists of nine separate integrations. Each integral may be evaluated by contour integration in the upper half of the complex ξ plane shown in Fig. 3. The remaining integration over k is considerably simplified by assuming $a/H\gtrsim 6$. The details of these integrations are extensive and will not be displayed here. The approximate expression for the

energy flux is

$$\overline{pw} \approx (4\pi aT)(\beta^2 N^2 T/2\pi\Gamma^3)\left\{\left[(\Gamma\Delta Z/2)\left(1+\tfrac{1}{2}e^{-\Gamma\Delta Z}+2\frac{g\Gamma}{N^2}\left(1+\frac{1}{2}\frac{g\Gamma}{N^2}\right)\right)\right.\right.$$

$$-\frac{3}{4}\left(1+\frac{4}{3}\frac{g\Gamma}{N^2}\right)(1-e^{-\Gamma\Delta Z})\Big](1-e^{-4\Gamma a/NT})-(NT/4\Gamma a)\left[\frac{3}{4}\Gamma\Delta Z\left(1+\frac{4}{3}\frac{g\Gamma}{N^2}\right)+\tfrac{4}{3}\pi^{-\frac{1}{2}}(\Gamma\Delta Z)^{\frac{3}{2}}e^{-\Gamma\Delta Z}\right.$$

$$\times\left[\frac{8}{35}(\Gamma\Delta Z)^2 M(4,9/2,\Gamma\Delta Z)-\frac{8}{5}\Gamma\Delta Z(\tfrac{1}{3}\Gamma\Delta Z+g\Gamma/N^2)M(3,7/2,\Gamma\Delta Z)\right.$$

$$\left.\left.+[\tfrac{1}{3}(\Gamma\Delta Z)^2+(2g\Gamma/N^2)(\Gamma\Delta Z+g\Gamma/2N^2)]M(2,5/2,\Gamma\Delta Z)\right]\right][1-(1+4\Gamma a/NT)e^{-4\Gamma a/NT}]$$

$$\left.+\text{terms proportional to } (NT/4\Gamma a)^2+\text{terms proportional to } e^{-2\Gamma z_1},\ e^{-2\Gamma z_2},\text{ and } e^{-\Gamma(z_1+z_2)}\right\}, \quad \text{(B9)}$$

where $M(a,b,x)$ denotes Kummer's function (Slater, 1964), and the terms which have not been written out explicitly in (B9) are, respectively, one and two orders of magnitude less than the leading terms.

REFERENCES

Akasofu, S.-I., 1963: The dynamic morphology of the aurora polaris. *J. Geophys. Res.*, **68**, 1667–1673.

——, 1964: The development of the auroral substorm. *Planetary Space Sci.*, **12**, 273–282.

——, 1965: Dynamic morphology of auroras. *Space Sci. Rev.*, **4**, 498–540.

——, S. Chapman and C.-I. Meng, 1965: The polar electrojet. *J. Atmos. Terr. Phys.*, **27**, 1275–1305.

Belon, A. E., G. J. Romick and M. H. Rees, 1966: The energy spectrum of primary auroral electrons determined from auroral luminosity. *Planetary Space Sci.*, **14**, 597–615.

Boström, R., 1964: A model of the auroral electrojets. *J. Geophys. Res.*, **69**, 4983–4999.

Cole, K. D., 1962: Joule heating of the upper atmosphere. *Australian J. Phys.*, **15**, 223–235.

Eckart, C., 1960: *Hydrodynamics of Oceans and Atmospheres*. New York, Pergamon Press, 290 pp.

Eliassen, A., and E. Palm, 1961: On the transfer of energy in stationary mountain waves. *Geophys. Publikasjoner*, **22**, 23 pp.

Friedman, J. R., 1966: Propagation of internal gravity waves in a thermally stratified atmosphere. *J. Geophys. Res.*, **71**, 1033–1054.

Hendl, R. G., 1968: The auroral electrojet: A review of the theories and an estimation of its role in the heating of the upper atmosphere in the polar regions. Master's thesis, Dept. of Astro-Geophysics, University of Colorado, 81 pp.

Heppner, J. P., 1954: Time sequences and spatial relations in auroral activity during magnetic bays at College, Alaska. *J. Geophys. Res.*, **59**, 329–338.

Hess, S. L., 1959: *Introduction to Theoretical Meteorology*. New York, Holt, Rhinehart and Winston, 362 pp.

Hines, C. O., 1964: Minimum vertical scale sizes in the wind structure above 100 kilometers. *J. Geophys. Res.*, **69**, 2847–2848.

——, 1965: Dynamical heating of the upper atmosphere. *J. Geophys. Res.*, **70**. 177–183.

Kim, J. S., and R. A. Volkman, 1963: Thickness of zenithal auroral arc over Fort Churchill, Canada. *J. Geophys. Res.*, **68**, 3187–3190.

King, G. A. M., 1966: The ionospheric disturbance and atmospheric waves, I. *J. Atmos. Terr. Phys.*, **28**, 957–963.

Lindzen, R. S., 1967: Thermally driven diurnal tide in the atmosphere. *Quart. J. Roy. Meteor. Soc.*, **93**, 18–42.

Mackie, A. G., 1965: *Boundary Value Problems*. New York, Hafner Publishing Co., 252 pp.

Maeda, M., and T. Watanabe, 1964: Pulsating aurorae and infrasonic waves in the polar atmosphere. *J. Atmos. Sci.*, **21**, 15–29.

Maggs, J. E., and T. N. Davis, 1968: Measurements of the thickness of auroral structures. *Planetary Space Sci.*,**16**, 205–209.

Nagata, T., 1950: On the auroral zone current. *Rept. Ionosphere Res. Japan*, **4**, 87–101.

——, 1962: Polar magnetic storms, especially in the southern polar region. *J. Phys. Soc. Japan*, **17**, Suppl. A-1, *Intern. Conf. Cosmic Rays and the Earth Storm*, 157–164.

Ogura, Y., and N. A. Phillips, 1962: Scale analysis of deep and shallow convection in the atmosphere. *J. Atmos. Sci.*, **19**, 173–179.

Pitteway, M. L. V., and C. O. Hines, 1963: The viscous damping of atmospheric gravity waves. *Can. J. Phys.*, **41**, 1935–1948.

Rees, M. H., and J. C. G. Walker, 1968: Ion and electron heating by auroral electric fields. *Ann. Geophys.*, **24**, 193–199.

Scrase, F. J., 1967: The electric current associated with polar magnetic substorms. *J. Atmos. Terr. Phys.*, **29**, 567–579.

Slater, L. J., 1964: Confluent hypergeometric functions. *Handbook of Mathematical Functions*, Washington, D. C., U. S. Government Printing Office, 1046 pp.

Thomas, G. E., 1967: Analytic solutions of the heat conduction equation in the thermosphere. Rept. TR-0158(3260-10)-3, Aerospace Corp., Los Angeles, Calif., 56 pp.

U. S. Standard Atmosphere, 1962: Washington, D. C., U. S. Government Printing Office, 278 pp.